

The Efficiency of Nanohydroxyapatite Granules on Bone Regeneration: Radiographic and Histopathologic Study in a Canine Model

Shaaban M. Gadallah¹, Mahmoud M. Mohamed^{1*}, Adel Al Akraa², Ahmed Sharshar¹, Mohamed El-Sunsafty¹

1 Department of Surgery, Anesthesiology and Radiology, Faculty of Veterinary Medicine, University of Sadat City.

2 Department of Surgery, Anesthesiology and Radiology, Faculty of Veterinary Medicine, Benha University, Egypt

*Corresponding author: drmahmoudvet@yahoo.com Received: 2/8/2024 Accepted: 27/9/2024

ABSTRACT

The primary factors leading to bone loss are trauma, tumor excision, and degeneration. Ongoing research has focused on investigating the efficacy of natural and synthetic substitutes for bone grafts, utilizing both in vivo and in vitro experiments. This study aimed to assess the efficacy of nano-hydroxyapatite (N-HA) in stimulating bone regeneration in significant bone defects in the tibia of dogs. This study utilized a cohort of 12 adult male mongrel dogs. Two holes with a diameter of 10 mm were surgically created in the upper region of the tibial bone. One defect was filled with Nano-HA powder, while the other defect was left unfilled. The advancement of N-HA's healing process was monitored through sequential radiographic imaging and histological examination until the completion of each designated observation period. The findings of our investigation demonstrated that the region where N-HA was inserted exhibited enhanced bone formation, suggesting a more rapid and robust healing reaction in comparison to the control site. The data presented here provide empirical evidence supporting the notion that Nano-HA possesses favorable biocompatibility, biodegradability, and osteoinductive properties.

Keywords: Bone graft, Dog, Gap defect, Nano-hydroxyapatite, Nanoparticles, substitute

INTRODUCTION

The cellular structure of bone tissue is peculiar and intricate. When damaged, it has a commendable ability to regenerate itself under normal conditions. (Schmidt-Bleek et al., 2014). Orthopedists may face significant challenges while attempting to cure later

deformities resulting from tumor removal, severe trauma, prolonged unions and nonunion, osteotomies, and arthrodesis. Surgical fixation with bone regeneration plans may be necessary to stimulate bone repair (Ragetyly & Griffon, 2011; Westhauser et al, 2016, Stanovici et al, 2016; Schemitsch,

2017). Fresh autografts are viewed as the most advantageous option for the repair of bone defects due to their high osteogenic potential. However, their availability in terms of quantity, shape, size, and the process of collection can lead to longer operative times and increased morbidity rates. Bone grafts can be sourced from a variety of living and non-living sources (Kim et al, 2009; De Grado et al., 2018). The utilization of allografts and xenografts, along with the decrease in donor morbidity rates, has resulted in an abundant supply of graft materials (Heo, et al. 2011; Yamada & Egusa, 2018). However, the practical use of this treatment is often impeded by the potential for immune rejection (also known as foreign body reaction) and the transmission of pathogens (Graham, et al 2010; Nandi, et al, 2010, Giannoudis, et al 2011; Herberts et al., 2011; De Grado et al., 2018).

Several biomaterials have been used and evaluated as bone substitutes (Nandi et al, 2010; Pilipchuk et al., 2015; Dorati et al., 2017; Wang and Yeung, 2017; Ghassemi et al., 2018). It exhibits the benefits of strong osteoconductivity, abundant accessibility, and excellent biocompatibility (Rahaman et al, 2011). Furthermore, a significant number of these materials exhibit specific mechanical characteristics that are essential for bone reconstruction (Pilipchuk et al., 2015). Alternatively, when used independently, the majority of currently available bone substitutes do not possess the osteoinductive and osteogenic characteristics necessary to repair bone lesions of a crucial magnitude (Ajeesh, 2010) Biomaterials are commonly categorized into three primary groups: bioactive ceramics, polymeric biomaterials, and composites. Bioactive ceramics can be derived from natural or synthetic origins. Instances of synthetic bioactive ceramics encompass

calcium silicate, hydroxyapatite (HA), tricalcium phosphate (TCP), and biphasic calcium phosphate (BCP) (ZHENG et al., 2023). One of the bioactive ceramics that has been studied extensively is hydroxyapatite. It makes up over 70% of the bulk of both bones and tooth enamel. Scaffolds, blocks, or granules made of it have found extensive use in bone restoration due to its chemical properties, biocompatibility, bioactivity, osteoconductivity, and structural and compositional similarity to the mineral phase of human bone hard tissue (Mahabole, 2012; Yelten and Yilmaz, 2017; Li, et al 2019). In order to improve X-ray imaging quality, resorption rates, durability, and the likelihood of migration from the recipient location, artificial HA has been extensively used as a replacement for natural HA. (Rajendran et al., 2014). HA has been effectively utilized alone or in combination with mesenchymal stem cells for restore critical-sized defect of bone tissue in vivo (Sekiya et al., 2002; Charlena, 2017; El-Bahrawy et al., 2021). The mechanical, bioactive, and architectural durability of nano-phase hydroxyapatite is much higher than that of conventional hydroxyapatite (HA). In contrast to more traditional forms, its surface is quite similar to trabecular bone. Furthermore, the surface area to volume ratio is greatly enhanced in nanophase materials due to the smaller particle size (Sullivan et al., 2014; Hu, et al 2015; Wang, et al 2017). Joint replacement and fibrous encapsulation are both reduced when this technique is used in bone grafting, along with significant osteoblastic adhesion and activity (Webster and Ahn, 2007; Gürbüz et al 2023). The researchers in this study set out to determine if N-HA could successfully fill in artificially produced critical size bone gap defects in a canine model, therefore eliminating the need for bone transplants.

MATERIALS AND METHODS

Nano-hydroxyapatite preparation

N-HA utilized was sourced from the Cytotoxicity Lab at the Faculty of Nanotechnology for postgraduate Studies, located at Cairo University, Sheikh Zayed. The specimens were processed through the technique of sonicated infusion to extract nanoparticles, using sonication prop at an intensity of 85% amplitude with pulses occurring every 1 second, for a duration of 30 minutes. Subsequently, the particles were supplemented with 50 microns to meet TEM grade guidelines and left to air dry for a period of five hours (Youssef, 2021). A high-resolution transmission electron microscope (HRTEM, JEOL TEM-2100, Japan) was used to examine its features, revealing its form and texture at a magnification of 20 X and an accelerating voltage of 250 KV. Every one of the 57×130 mm Self-Sealing Sterilization Pouches included 0.5 gram of N-HA. We used UV light for 10 minutes to sterilize the material.

Animal model and housing:

The Animal Care and Use Committee University of Sadat City–Faculty of Veterinary Medicine, located at Sadat City, Egypt. approved all actions. This study required the participation of twelve adult male mongrel dogs that were in excellent physical condition. The animals had an average age of 3 ± 1 year, and their weight ranged from 15 to 25 kg. Prior to the start of the experiment, the animals were kept separately and given a two-week time to adapt. All dogs had treatment for both internal as well as external parasites. The animals were fed commercially-manufactured dog food that followed

traditional methods. During the entirety of this study, the animals had unlimited access to food and water. The dogs were classified into four equitably divided groups according to the length of observation, which were 2, 4, 12, and 24 weeks.

Surgical procedure

All dogs were pre-medicated with intravenous injection of mixture of atropine sulfate 0.05 mg/kg (Atropine sulfate®: 1mg/ml Adwia company, located in Egypt) and xylazine hydrochloride 1 mg/kg (Xylaject®: 2% sol. Adwia company, located in Egypt). Anesthesia was induced through intravenous injection of Ketamine hydrochloride 10 mg/kg (Ketalar®: 5% sol. Amoun company, located in Egypt). The anesthetic depth was maintained with intravenous administration of 2.5 % thiopental sodium (Thiopental®: EPICO Co., located in Egypt) (Schmidt et al., 1995). The inside region of the right thigh was sterilized and then shielded with a sterile sheet. A ten centimeter skin incision was made on the medial surface to expose the bone. The incision included the skin, subcutaneous tissue, and periosteum. The incision started at the juncture of the highest portion of the tibial tuberosity and proceeded in a downward direction two holes with a diameter of 10 mm were made using a sterile drill bit with a diameter of 10 mm. The holes were formed at the proximal third and were 1 cm apart. The drilling process was done under continuous irrigation with sterile saline. Each hole flw penetrated just one cortex. The bleeding from the holes was controlled by placing a sterile gauze pack. In all dogs, the first hole closest to the body was filled with 0.5 grams of N-HA, whereas the second hole was left unfilled as a control (Figure 1). Polyglactin 910 was used to suture and close the surgical

wound (Vicryl®). The operated animals received antibiotic course contains Cefotaxime sodium at dose of 4.5 mg/kg

b.w. every eight hours for five successive days. The skin sutures were detached ten days post-operation.



Figure 1: A surgical picture is shown, depicting (A) a skin incision done on the inside side of the upper part of the tibia. The N-HA powder was implanted in the proximal hole (B), while the second hole was left empty as a control.

Post-operative follow-up evaluations Radiographic Examination:

Radiographic projections of the tibia were taken from a medio-lateral perspective at various time intervals. Immediately after the surgery (day zero) and then at the 2nd, 4th, 12th, and 20th weeks post-surgery. The radiographs were assessed to determine the radiographic density at each hole and the amount of new bone growth.

Histopathologic Evaluation:

At the conclusion of each designated time frame (2, 4, 12, and 20 weeks), three dogs were subjected to euthanasia. The surgically treated tibiae were collected and inspected visually. Every imperfection was examined to see whether it was completely or partially filled in comparison to the surrounding bone. Specimens of bone blocks were extracted from the implanted region of both tibiae. The bone blocks were decalcified by using formic acid at a concentration of 10% until complete decalcification was obtained. After decalcification, the samples were cut, washed with water, dehydrated using progressively higher concentrations of ethyl alcohol, clarified with xylene, and ultimately embedded in paraffin. A 4-6 μ thin slice was created and subjected to Hematoxylin & Eosin staining in order to facilitate histological investigation (Bancroft, 2008).

RESULTS

Electron microscopic scanning of the nano-hydroxyapatite

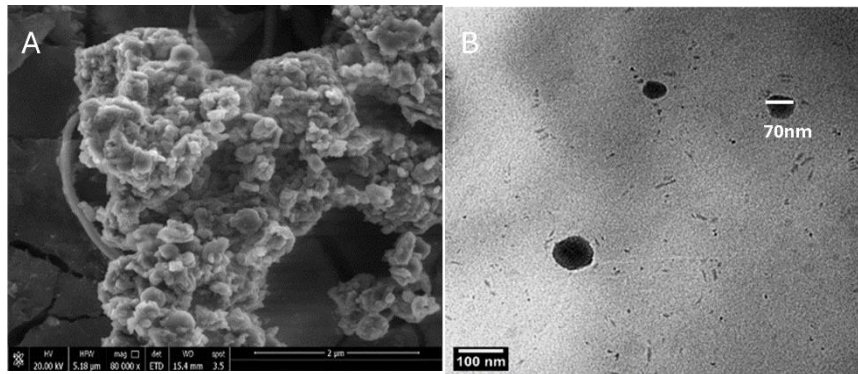


Figure 2: Displaying Scanning electron microscopy (SEM) was employed to observe the nanoparticles of the composites and analyze their structure and shape (A). The Transmission Electron Microscope (TEM) revealed the presence of nano-sized spheres measuring 70nm in diameter.

Sequential radiographic results:

Following the surgery, the holes filled with Nano-HA material were visibly opaquer when compared to the control hole (Fig. 3). At the conclusion of the second week, the hole that had been implanted with N-HA exhibited almost total absorption of the inserted materials in its core, resulting in a radiolucent appearance, with only a tiny radiopaque zone at the periphery (Figure 4A). By the conclusion of the fourth week, a noticeable rise in the density of the neighboring region in which Nano-HA had been introduced was evident, with the density showing a higher value as it approached the central area. In contrast, the control group exhibited no observable changes in comparison to the previous period of observation (Figure 4B). By the

conclusion of the 12th week following the surgical procedure, a noticeable augmentation in radiodensity was detected at the site where Nano-HA was implanted in comparison to the earlier observation, although it remained less radiopaque when compared to the surrounding bone tissue. Conversely, the control site exhibited a minor elevation in radiodensity at its outer edges, while the central portion continued to display complete radiolucency (see Figure 4C). Although the control hole's width had significantly shrunk by the end of the monitoring period (20 weeks after the operation), its radiolucent core allowed for easy radiography identification. As opposed to the surrounding host bone, the majority of the holes treated with Nano-HA disappeared and had a uniformly radiodense appearance (Figure 4D).



Figure 3: displaying a radiograph of the operated tibia just after the procedure. It should be noted that the hole where Nano-HA (1) was implanted looked radiodenser, matching the surrounding host bone. It seems that the control hole (2) is entirely radiolucent.

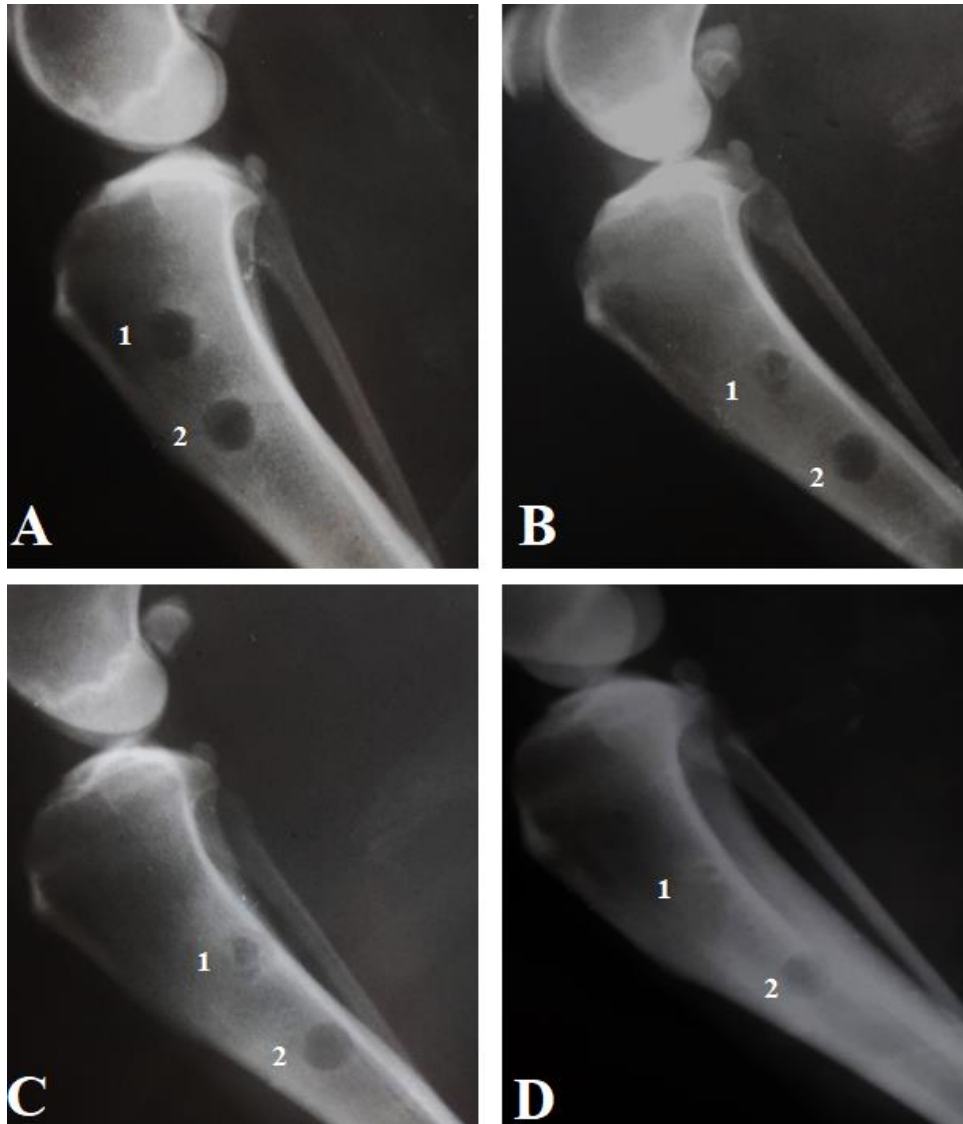


Figure 4: sequential radiography of the operated tibia during the observation period at 2-weeks (A), 4-weeks (B), 12-weeks (C), and 20-weeks (D) post-operation. upper hole implanted with Nano-HA while the lower is the control (empty). Note: the progressive increase of the radiodensity at the hole implanted with Nano-HA, which started at the periphery of the hole and increased toward the center. The control hole appeared radiolucent though out the whole observation period.

Histopathology Evaluation:

Microscopical examination of bone samples collected from control group euthanized after 2, 4 and 12 weeks. Afterward showed that, the entire bone holes were filled with collagen bundles and cellular infiltration (Figure 5A, B, C). After 20 weeks, control bone holes begin to form immature bone (woven bone, WB) at the margin and

connective tissue at the center of the wound (Figure 5D). Bone holes treated with Nano-HA exposed that the entire bone holes were sealed with collagen bundles freshly formed capillaries at 2 weeks. Afterwards (Figure 5E). At the 4th weeks post-operation, the collagen bundles become organized and mixed with immature bone (WB) cells with obvious osteoblastic and osteoclastic

activity (Figure 5F). At twelve weeks post-operation, the amount of the newly constructed immature bone cells improved and become prominent with disposition of soft callus which filled most of the hole (Figure 5G). By the end

of the observation period (20 weeks post-operation), a well-developed mature bone matrix (compact bone) mixed with remnant of immature bone matrix were detected (Figure 5H).

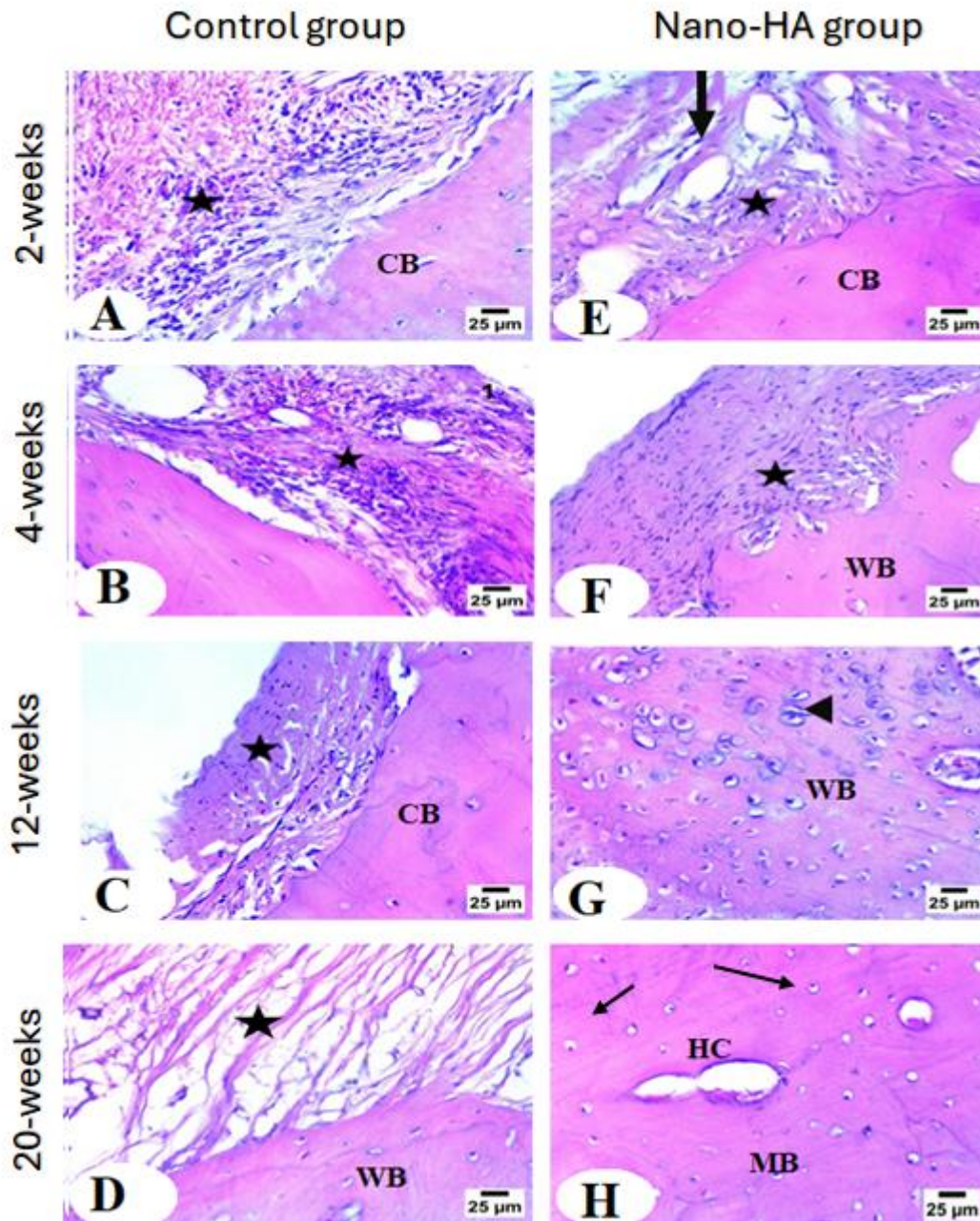


Figure 5: Dog tibia. A, B, C, and D representing the control holes at 2-, 4-, 12-, and 20-weeks post-operation respectively, showing collagen bundles filled the entire hole (asterisks). Only a small amount of undeveloped bone (WB) was created at the periphery of the hole by the completion of the observation period (D). E, F, G, and H representing the Nano-HA treated hole at 2-, 4-, 12-, and 20-weeks Afterwards respectively, display that the entire hole occupied with organized fibrous connective tissue (asterisk) with newly molded capillaries (arrows) be the end of the 2nd week Afterwards (E). By the end

of the 4th week Afterwards (F) a newly formed immature bone (WB) was formed at the periphery of the hole. By the end of the 12th week Afterwards (G), the entire hole filled with immature bone cells (arrow head) and immature bone (WB). By the end of the observation period (H), the entire hole filled with well-formed mature bone (MB) in between remnant of immature bone. H &E stain, X 10.

DISCUSSION

Numerous techniques have been utilized to reconstruct bone, especially when there is a sizable amount of bone loss (Torrioni, 2009; Kim et al., 2009; Nandi et al., 2010; Heo et al., 2011). The current techniques are addressed toward improvement of the bone ability to regenerate itself. For this purpose, various types of biomaterials have been examined. They can eliminate most of the reported disadvantages of auto, allo, and xenografts in terms of infection, availability, and donor site morbidity. However, they still lack the ideal properties of autografts, which is the presence of viable cells (El-Bahrawy, et al 2021; Tawfeek et al., 2023). Hydroxyapatite is one of the most often utilized biomaterials, whether in its conventional or nano-form. Synthetic hydroxyapatite is the least soluble and most stable kind of calcium phosphates (CaPs) as compared to its natural form. Like a natural hunger, which is what makes up bone's mineral makeup (Bal, et al.2020).

In recent times, advancements in nanotechnology have improved the bioactivity of hydroxyapatite crystals, resulting in a more favorable response when interacting with nanocrystals as opposed to larger crystals (Wang et al 2017). The nano-phase hydroxyapatite has structural and surface properties alike to that of human and animal bone. And provides as the primary component responsible for imparting bone rigidity. In addition, its nano-size provides instant integration with host bone due to its larger surface area (Sullivan et al.,

2014). In this study, Nano-HA was specifically selected, and we have focused in evaluating its capability to induce new bone formation when used to reconstruct critical size gap defects in the canine tibia. We assume that Nano-HA could be a good bone graft substitute.

In this study the used hydroxyapatite nanoparticles were evaluated using TEM. Our results revealed that it appeared as agglomerated spheres with (70) nm average particle size. According to (Youssef et al., 2011), this particle size is an optimum for a bone substitute. Hu, et al (2015) analyzed the morphologic relations between nano-hydroxyapatite particles and the amount of new bone formation. According to their findings, nano-hydroxyapatite favored cell adhesion and osteogenic differentiation, as evidenced by an increase in osteogenic gene expression, an increase in alkaline phosphatase activity, and an increase in osteopontin production.

In this study, the behavior and the healing pattern of the Nano-HA have been evaluated using sequential radiographic and histopathological examination. By the end of the observation period the Nano-HA implanted hole completely vanished and couldn't be detected radiographically compared to the control one. The histological findings complimented the radiological results which indicated new bone formation in the hole implanted. Directly after the implantation, and comparing to the control holes, the

Nano-HA implanted holes emerged homogeneously dense with the surrounding host bone. Similar outcomes have been described by (Rajendran et al., 2014; El-Bahrawy, et al 2021). By the end of the 2nd week afterwards a complete resorption of the Nano-HA was stated leaving the defect area entirely radiolucent. The result is compatible with that previously mentioned by (Meskinfam et al., 2018), who asserted that Nano-HA marked by rapid absorbability compared to its conventional counterpart. On the contrary, this resorption rate and pattern greatly differs than that reported by (El-Bahrawy et al., 2021) The informant reported that the Nano-HA particles exhibited a prolonged absorption rate in the body, persisting for a duration of 16 weeks following the implantation. During the next observation period, the X-ray picture of the Nano-HA implanted holes showed a substantial increase in radiodensity, starting from the outside edge and advancing towards the center of the hole. At the end of the 20th week of monitoring, most of the faulty region had disappeared, and the implanted area showed a consistent density compared to the surrounding host bone. This signifies the formation of fresh bone, regardless of its characteristics. The data presented here contradict the findings published by El-Bahrawy, et al (2021), the authors observed that the spaces implanted with Nano-HA and the embedded materials stayed discernible on radiographs up to the 16th week following implantation. The disparity in the pace and pattern of absorption seen in the two trials may likely be ascribed to the methodology employed in the preparation of Nano-HA and its inherent physical characteristics.

Our histological verdicts corroborated the previously documented radiological findings. The presence of active

osteogenesis and the beginning of new bone formation were observed within the Nano-HA cavities, in contrast to the control holes where bone growth did not occur throughout the whole observation period. The process of bone production and growth becomes highly visible at the implanted holes treated with Nano-HA, reaching a mature condition by the end of the 20th week, with significant progress observed as early as the 4th week. The examination revealed significant enlargement of the cartilage cells (chondrocytes) and the development of a kind of bone called woven bone, accompanied by the presence of fibrous tissue. The positive outcome may be attributed to the osseointegration and osteoinductive properties of Nano-HA granules, which promote the growth and attachment of bone cells (osteoblasts) and facilitate the rapid formation of calcium-containing minerals on the surface of the implant. (Von Doernberg et al., 2006). The observed occurrences can be ascribed to the advantageous characteristics of biocompatibility, biodegradability, and bioactivity exhibited by Nano-hydroxyapatite crystals (Martino et al., 2005; Zhang, et al., 2023). The presence of fully developed bone, together with traces of less developed bone, in the Nano-HA implanted hole indicates the high quality of the newly formed bone. From the author's viewpoint, extending the period of observation or incorporating supplementary materials can improve the quality of freshly formed bone by stimulating the growth and movement of cells.

CONCLUSION

Nano-Hydroxyapatite (Nano-HA) demonstrates favorable biocompatibility, biodegradability, and osteoinductivity, leading to its application as a bone graft substitute.

REFERENCES

- Dorati, R., DeTrizio, A., Modena, T., Conti, B., Benazzo, F., Gastaldi, G., & Genta, I. (2017). Biodegradable scaffolds for bone regeneration combined with drug-delivery systems in osteomyelitis therapy. *Pharmaceuticals (Basel)*, 10
- Wang, W and Yeung, K.W.K. 2017. Bone grafts and biomaterials substitutes for bone defect repair: A review. *Bioactive Materials*. 1-24.
- Ghassemi, T., Shahroodi, A., Ebrahimzadeh, M. H., Mousavian, A., Movaffagh, J., & Moradi, A. (2018). Current concepts in scaffolding for bone tissue engineering. *The Archives of Bone and Joint Surgery*, 6, 90–99.
- Rahaman, M.N., Day, D.E., Bal, B.S., Fu, Q., Jung, S.B., Bonewald, L.F., Tomsia, A.P. 2011. Bioactive glass in tissue engineering. *Acta Biomaterialia* 7: 2355–2373
- Ajeesh, M., Francis, B.F., Annie, J., Harikrishna Varma P, R. 2010. Nano iron oxide-hydroxyapatite composite ceramics with enhanced radiopacity. *J Mater Sci Mater Med* 21: 1427-1434,
- Abels, E.; Breakefeld, X.(2016): Introduction to extracellular vesicles: biogenesis, RNA cargo selection, content, release, and uptake. *Cell Mol Neurobiol*. 36:301–12.
- Bal, Z.; Kaito, T.; Korkusuz, F.; Yoshikawa,H. (2020): Bone regeneration with hydroxyapatite-based biomaterials, Qatar University and Springer Nature Switzerland AG , 3:521–544.
- Bancroft, J.D.(2008): Theory and Practice of Histological Techniques. Elsevier Heal Sci. UK.;6th Edn
- Bucki, R.; Bachelot-Loza, C.; Zachowski, A.; Giraud, F.; Sulpice, J.(1998): Calcium induces phospholipid redistribution and Microvesicle release in human erythrocyte membranes by independent pathways. *Biochemistry*;37(44):15383–15391. 10.1021/bi9805238.
- Charlena; Bikharudin,A.; Tri Wahyudi, S. ; Erizal (2017): Synthesis and characterization of hydroxyapatite-collagen-chitosan (ha/col/chi)composite by using ex-situ wet precipitation method, *Rasayan J. Chem.*, 10(3), 766-770.
- Crawford, S.; Diamond, D.; Brustolon, L.; Penarreta, R. (2010): Effect of increased extracellular ca on microvesicle production and tumor spheroid formation. *Cancer Microenviron.*;4(1):93–103. 10.1007/s12307-010-0049-0
- De Grado, G. F., Keller, L., Idoux-Gillet, Y., Wagner, Q., Musset, A. M., Benkirane-Jessel, N., Offner, D. (2018). Bone substitutes: A review of their characteristics, clinical use, and perspectives for large bone defects management. *Journal of Tissue Engineering*, 9,
- D’Souza-Schorey, C.; Clancy, J. (2012): Tumor-derived Microvesicles: shedding light on novel microenvironment modulators and prospective cancer biomarkers. *Genes Dev.*,26(12):1287–1299. 10.1101/gad.192351.112.
- Elahi, F.; Farwell, D.; Nolta, J.; Anderson, J.(2020): Preclinical translation of exosomes derived from mesenchymal stem/stromal cells. *Stem Cells*.38:15–21.
- El-Bahrawy, A.; El-Hamadan, S.; Sharshar, A.; El Ballal, S. (2021): Comparative Evaluation of Bone Regenerating Capacity Using Nanocrystalline Hydroxyapatite and Coral Composite: A Canine Model Study, *Journal of Current Veterinary Research*, 2636-4026
- Gürbüz, S.;Doğan, A.; Karakeçili, A.; Toközlü, B.(2023): In vivo behavior of a collagen-coated nano-hydroxyapatite enriched polycaprolactone membrane in rat mandibular defects , *Ulus Travma*

Acil Cerrahi Derg, October 2023, Vol. 29, No. 10.

Giannoudis P.; Faour, O. Goff, T, Kanakaris, N. ;Dimitriou, R. (2011):Masquelet technique for the treatment of bone defects: tips-tricks and future directions. *Injury* 2011 42 591–598

Graham, S. ;Leonidou, A.; Aslam-Pervez, N. et al(2010): Biological therapy of bone defects: the immunology of bone allotransplantation, *Expert Opin Biol Ther* 10:885–901.

Harding, C.; Stahl, P.(1983): Transferrin recycling in reticulocytes: pH and iron are important determinants of ligand binding and processing. *Biochem Biophys Res Commun* ;113:650–8.

Heo, S.H., Na, C.S. and Kim N.S. 2011. Evaluation of equine cortical bone transplantation in a canine fracture model. *J. Veterinarni. Medicina*, 56, 3: 110-118.

Herberts, C.A., Kwa, M.S.G., Hermsen, H.P.H. 2011. Risk factors in the development of stem cell therapy. *Journal of Translational Medicine* 9, 29. <http://dx.doi.org/10.1186/1479-5876-9-29>

Hu, J.; Yang, Z.; Zhou, Y.; Liu, Y.; Li, K.; Lu, H.(2015):Porous biphasic calcium phosphate ceramics coated with nano-hydroxyapatite and seeded with mesenchymal stem cells for reconstruction of radius segmental defects in rabbits. *J. Mater. Sci. Mater. Med.*, 26, 257

Jain, K. (2011): *Comprehensive biotechnology*. 2nd ed. Academic Press: Burlington; p. 599–614.

Jia, Y.; Zhu, Y.; Qiu, S.; Xu, J.; Chai, Y.(2019): Exosomes secreted by endothelial progenitor cells accelerate bone regeneration during distraction osteogenesis by stimulating angiogenesis. *Stem Cell Res Ther.* 10:1–13.

Kakade, P.; Zope, S. ; Suragimath, G.; Varma, A.; Pisal A. (2021): hanging Trends in use of Bone Grafts and Bone Grafts Substitutes for Periodontal Regeneration / *Trends Biomater. Artif. Organs*, 35(2), 222-228.

Kim, D.H., Rhim R, Li L, Martha J, Swaim BH, Banco RJ, et al. 2009. Prospective study of iliac crest bone graft harvest site pain and morbidity. *Spine J*;9 11 886–92.

Li, N.; Wu, G.; Yao, H.; Tang, R.; Gu, X.; Tu, C. (2019): Size effect of nano-hydroxyapatite on proliferation of odontoblast-like MDPC-23 cells. *Dent. Mater. J.*, 38, 534–539.

Mahabole, M.; . Bahir, M.; Kalyankar, N. ; Khairnar ,R. (2012): Effect of incubation in simulated body fluid on dielectric and photoluminescence properties of nano-hydroxyapatite ceramic doped with strontium ions, *Journal of Biomedical Science and Engineering*, 5, 396.

Martino, A., Sittinger, M. and Risbud, M.V. 2005. Chitosan: a versatile biopolymer for orthopaedic tissue-engineering. *Biomaterials*, 26(30):5983-5990.

<https://doi.org/10.1016/j.biomaterials.2005.03.016>

Meskinfam, M., Bertoldi, S., Albanese, N., Cerri, A., Tanzi, M,C., Imani, R., Baheiraei, N., Farokhi, M., Farè S. (2018): Polyurethane foam/nano hydroxyapatite composite as a suitable scaffold for bone tissue regeneration. *Materials Science and Engineering C*, 82:130-140.

Nandi, S.K., Roy, S., Mukherjee, P., Kundu, B., De, D.K. & Basu, D. 2010. Orthopaedic applications of bone graft &graft substitutes: a review.*Indian J Med Res* July,132, pp 15-30 Younger, EM., Chapman, MW. 1989 Morbidity at bone graft donor sites. *J Orthop Trauma*; 3:192–5.

Pan, B.; Johnstone, R. (1983): Fate of the transferrin receptor during

- maturation of sheep reticulocytes in vitro: selective externalization of the receptor. *Cell*; 33:967–78.
- Pegtel, D.; Gould, S. (2019): Exosomes. *Annu Rev Biochem* ;88:487–514
- Phinney, D.; Pittenger, M. (2017): Concise review: MSC-derived exosomes for cell-free therapy. *Stem Cells Dayt Ohio.* ;35:851–8.
- Pilipchuk, S. P., Plonka, A. B., Monje, A., Taut, A. D., Lanis, A., Kang, B., & Giannobile, W. V. (2015). Tissue engineering for bone regeneration and osseointegration in the oral cavity. *Dental Materials*, 31, 317–338
- Rajendran, A., Barik, R.C., Natarajan, D., Kiran, M.S. and Pattanayak, D.K. 2014. Synthesis, phase stability of hydroxyapatite–silver composite with antimicrobial activity and cytocompatibility. *Ceramics International*, 40(7):10831-10838.
- Ragetly, G.; Griffon, D.(2011): The rationale behind novel bone grafting techniques in small animals, *Vet Comp Orthop Traumatol* 24:1–8.
- Schemitsch, E.(2017): Size matters: defining critical in bone defect size! *J. Orthop. Trauma* 31, S20–S22.
- Schmidt-Bleek K, Petersen A, Dienelt A, Schwarz C, Duda GN. 2014. Initiation and early control of tissue regeneration – bone healing as a model system for tissue regeneration. *Expert Opin Biol Ther* ;14 2 247–59.
- Sedgwick, A.; D’Souza-Schorey ,C.(2018): The biology of extracellular Microvesicles, *Wiley Traffic* 19:319–327.
- Stanovici, J. Le Nail, L.R., Brennan M.A., Vidal L., Trichet, V., Rosset P. Layrolle, P. 2016. Bone regeneration strategies with bone marrow stromal cells in orthopaedic surgery. *Current Research in Translational Medicine* 64, 83–90
- Sullivan MP, McHale KJ, Parvizi J, Mehta S. (2014): Nanotechnology: current concepts in orthopaedic surgery and future directions. *Bone Joint J* 2014; 96-B (5): 569-73.
- Tawfeek GA., Abdelgaber M., Gadallah S., Anis A., Sharshar A. (2023). A Novel Construct of Coral Granules-Poly-L-Lactic Acid Nanomembrane Sandwich Double Stem Cell Sheet Transplantation as Regenerative Therapy of Bone Defect Model. *Experimental and Clinical Transplantation* 2: 158-170
- Torroni A. 2009. Engineered bone grafts and bone flaps for maxillofacial defects: state of the art. *J Oral Maxillofac Surg*; 67: 1121-7.
- Von Doernberg, M.C., Von Rechenberg, B., Bohner, M., Grünenfelder, S., van Lenthe, G.H., Müller, R., Gasser, B., Mathys, R., Baroud, G. and Auer, J. 2006. In vivo behavior of calcium phosphate scaffolds with four different pore sizes. *Biomaterials*, 27(30):5186-98.
<https://doi.org/10.1016/j.biomaterials.2006.05.051>
- Wang, X.; Li, G.; Guo, J.; Yang, L.; Liu, Y.; Sun, Q.; Li, R.; Yu, W.(2017):Hybrid composites of mesenchymal stem cell sheets, hydroxyapatite, and platelet-rich fibrin granules for bone regeneration in a rabbit calvarial critical-size defect model. *Exp. Ther.Med.*, 13, 1891–1899
- Webster T.J., Ahn E.S. (2007): Nanostructured Biomaterials for Tissue Engineering Bone. In: Lee K., Kaplan D., editors. *Tissue Engineering II: Basics of Tissue Engineering and Tissue Application.* Springer; Berlin/Heidelberg, Germany: pp. 275–308.
- Westhauser, F., Hollig, M., Reible, B., Xiao, K., Schmidmaier, G., Moghaddam, A. 2016. Bone formation of human mesenchymal stem cells harvested from reaming debris is stimulated by low-dose bone

morphogenetic protein-7 application in vivo. *Journal of Orthopaedics* 13, 404–408.

Yelten, A. and Yilmaz, S. 2017. Comparison of Naturally and Synthetically Derived Hydroxyapatite Powders. *Acta Physica Polonica A*, 131(1):55-58

Youssef F, Mohamed G, Ismail S, et al. (2021): Synthesis, characterization, and in vitro antimicrobial activity of florfenicol-chitosan nanocomposite. *Egyptian journal of chemistry* 64(2): 941–948.).

Yamada, M., & Egusa, H. (2018). Current bone substitutes for implant dentistry. *Journal of Prosthodontic Research*, 62, 152–161.

Youssef F, Mohamed G, Ismail S, et al. (2021): Synthesis, characterization, and in vitro antimicrobial activity of florfenicol-chitosan nanocomposite. *Egyptian journal of chemistry* 64(2): 941–948.

ZHENG, J.; LU, X.; LU, Y.; LU, Y.; WANG, Y.; LU, J.(2023): Biological Mechanism and Application: Functional Biadaptability in Medical Bioceramics, *Journal of Inorganic Materials* 39(1):244.